DALTON
FULL PAPER

Copper(II) complexes of 6-hydroxymethyl-substituted tris(2-pyridylmethyl)amine ligands †

Zhicong He, P. Jinny Chaimungkalanont, Donald C. Craig and Stephen B. Colbran *

School of Chemistry, The University of New South Wales, Sydney, NSW 2052, Australia. E-mail: S.Colbran@unsw.edu.au

Received 6th January 2000, Accepted 13th March 2000

Three potentially tripodal, tris(2-pyridylmethyl)amine (tpa) ligands with hydroxymethyl substituents, [6-(hydroxymethyl)-2-pyridylmethyl]bis(2-pyridylmethyl)amine (HL^1), bis[6-(hydroxymethyl)-2-pyridylmethyl]-2-(pyridylmethyl)amine (H_2L^2), tris[6-(hydroxymethyl)-2-pyridylmethyl]amine (H_3L^3), have been prepared in good yields. From these ligands, the copper(II) co-ordination complexes $[Cu(HL^1)Cl]Cl$ **1**, $[Cu(H_2L^2)Cl]X$ (X = Cl **2** or *p*-toluenesulfonate **3**), $[Cu(L^2BF_2)][BF_4]$ **4** a complex of a novel macrocyclic anion with a tpa core, $[Cu(H_3L^3)Br_{0.43}Cl_{0.57}]_2[Cu(Br_{0.43}Cl_{0.57})_2(Br_{0.97}Cl_{0.03})_2]$ **5** with compositionally disordered bromo and chloro co-ligands, $[Cu(H_3L^3)Br]Br$ **6** and the unusual trimer $[Cu_3\{H_3(L^3)_2\}Br][BF_4]_2$ **7** have been synthesized and their spectroscopic and redox properties and crystal structures obtained.

Introduction

Transition metal complexes of tris(pyridylmethyl)amine (tpa) ligands and their derivatives have been much studied recently as models for the active sites of various metalloproteins.[1–4] Against this background lies the interest in the copper co-ordination chemistry of these ligands.[1,4–13] Many of the copper-containing proteins that the copper–tpa complexes are targeted to model have di- or tri-nuclear copper active sites and/or unusual and often redox-active cofactors.[14–16] Synthetic routes to metal complexes of multinucleating tpa ligands[7–10] and tpa ligands with cofactors attached to the pyridine ring(s)[9,10] are facilitated by functional groups on the pyridine ring(s). Towards the aim of preparation of multinucleating and cofactor substituted tpa ligands, we report here three novel tpa derivatives which bear one, two or three hydroxymethyl group(s), respectively, at the 6 position of the pyridine ring(s) and describe copper(II) complexes of these ligands. These hydroxymethyl-substituted tpa ligands offer scope for further elaboration and substantial differences are seen between their copper(II) complexes and those of simpler tpa ligands.

Results and discussion

Preparations

Ligands. Three new hydroxymethyl-substituted tpa ligands, HL^1, H_2L^2 and H_3L^3, were targeted, Scheme 1. All three ligands were prepared from 6-(bromomethyl)-2-(hydroxymethyl)-pyridine, which was obtained by routine syntheses,[17] starting from 2,6-dicarboxypyridine rather than from 2,6-di(hydroxymethyl)pyridine, which is expensive. Ligands HL^1 and H_2L^2 were prepared by slow addition of an acetonitrile solution of *N*,*N*-bis(2-pyridylmethyl)amine or 2-pyridylmethylamine and triethylamine to an acetonitrile solution of 6-(bromomethyl)-2-(hydroxymethyl)pyridine (1 equivalent for HL^1 and 2 equivalents for H_2L^2). Completion of the reactions was monitored by thin layer chromatography and typical reaction times were between two and three days. After work-up, HL^1 and H_2L^2 were obtained as clear yellow (85–95%) and light brown oils (60–75%), respectively. Larger scale preparations resulted in higher yields. This procedure, however, failed for the preparation of H_3L^3. Reaction of ammonium acetate and 6-(bromomethyl)-2-(hydroxymethyl)pyridine with triethylamine as the base in acetonitrile afforded 2-(hydroxymethyl)-6-(triethylammonium-methyl)pyridine bromide. Using sodium carbonate, rather than triethylamine, as the base in this reaction gave $H_3L^3{\cdot}x$NaBr in reasonable yield. The sodium content was ascertained by inductively coupled plasma atomic emission spectroscopy (ICP-AES) analysis and x for different preparations was found to vary between ≈2.4 and 3.4.

Elemental analyses were not obtained for the ligands. However, the successful preparations of the complexes below attest to their formulations and the ligands do show correct mass and NMR spectra. Briefly, the more important spectroscopic data are as follows. The EI mass spectrum of HL^1 shows peaks at *m*/*z* 321 (MH^+), 641 (M_2H^+) and 200 [$(NC_5H_4CH_2)_2N^+$], and the ^{1}H NMR spectrum in $CDCl_3$ shows signals corresponding to the pyridine protons between δ 7.07 and 8.53 along with a singlet at δ 4.72 for two methanol (CH_2OH) and δ 3.89 for six methylene ($NCH_2C_5H_4N$) protons. The UV/VIS absorption spectrum of HL^1 shows a band at 265 nm (ε = 9420 M^{-1} cm^{-1}) and the FTIR spectrum exhibits a broad O–H stretch at 3350 cm^{-1}. The EI mass spectrum of H_2L^2 reveals intense peaks at *m*/*z* 351 (MH^+) and 258 [$(M - CH_2C_5H_4N)^+$]. The ^{1}H NMR spectrum exhibits singlets at δ 3.87 and 4.73 for the methylene protons of pyridylmethyl and methanol groups respectively as well as pyridyl peaks between δ 7.06 and 8.53. This ligand also shows a prominent absorption in the UV/VIS spectrum at 264 nm (ε = 9910 M^{-1} cm^{-1}) and the most notable feature in its IR spectrum is the broad O–H band at 3300 cm^{-1}. Notably, the positive-ion electrospray mass spectrum of $H_3L^3{\cdot}x$NaBr exhibits an intense peak at *m*/*z* 403 for the cation, $[Na(H_3L^3)]^+$, consistent with the ligand binding strongly to sodium ion. No peaks corresponding to the ion $[Na(H_3L^3)_2]^+$ were observed, in contrast with tpa which gives $[Na(tpa)_2]^+$ with sodium ion in the ES mass spectrum.[18] The ^{1}H NMR spectrum is simple as expected and reveals pyridyl multiplets at δ 7.76, 7.44, and 7.30, and peaks for the methanol [δ 4.52 (CH_2) and 5.3 (OH)] and methylene (δ 3.74) protons. The UV/VIS spectrum of $H_3L^3{\cdot}x$NaBr shows a strong peak at 266 nm (ε = 11400 M^{-1}

† Electronic supplementary information (ESI) available: partial crystal structure of complex **5**, VIS/NIR spectra. See http://www.rsc.org/suppdata/dt/b0/b000092m/

DOI: 10.1039/b000092m

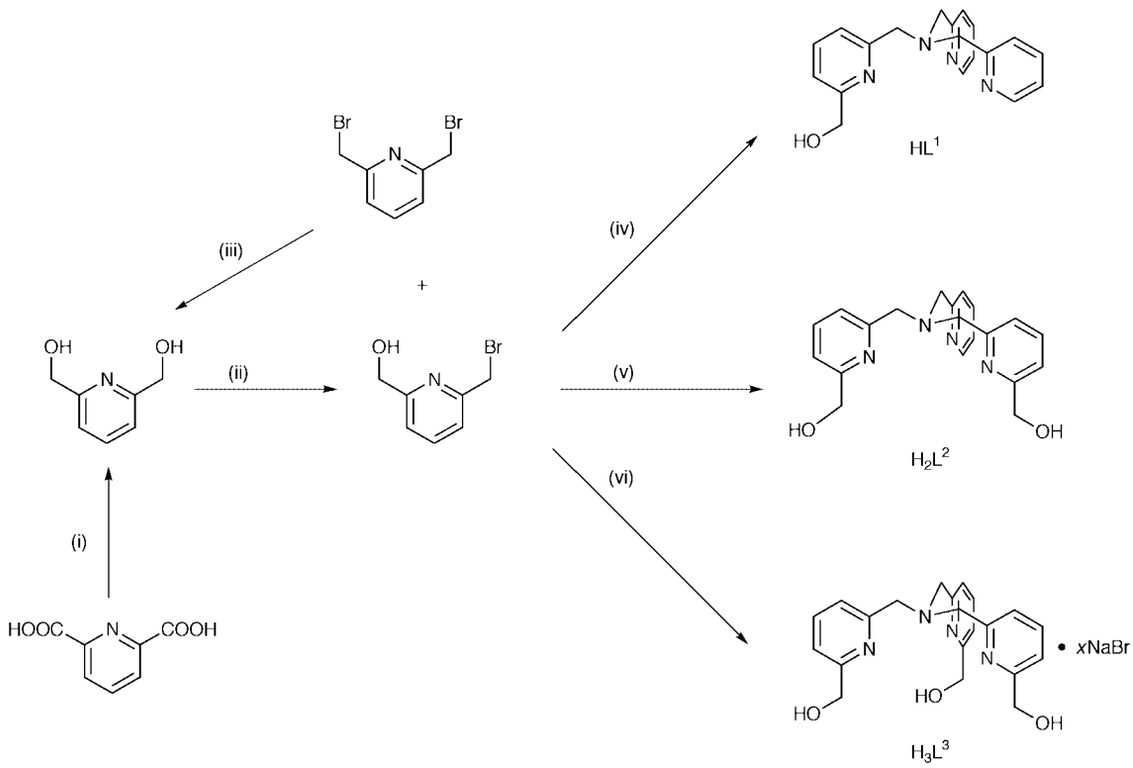

Scheme 1 (i) (a) Methanol, H^+; (b) $LiAlH_4$, yield 80% overall; (ii) 48% HBr, 45%; (iii) (a) water; (b) $NaHCO_3$, 95%; (iv) bis(2-pyridylmethyl)amine (1 equivalent), NEt_3, CH_3CN, 25 °C, 2–3 days, 95%; (v) (2-pyridylmethyl)amine (0.5 equivalent), NEt_3, CH_3CN, 25 °C, 2–3 days, 75%; (vi) NH_4OAc, Na_2CO_3, CH_3CN, 25 °C, 2–3 days, 60–70%.

cm^{-1}) and a broad O–H stretching vibration appears at 3368 cm^{-1} in the FTIR spectrum.

Compounds HL^1, H_2L^2 and H_3L^3 bear one to three hydroxymethyl functional groups, respectively, and therefore should prove to be useful precursors to a variety of new derivatised tpa ligands. To this end, the following test reactions were carried out on HL^1. Treatment of HL^1 in chloroform cooled to −5 °C with thionyl chloride afforded the 6-chloromethyl derivative of tpa, whereas in DMSO–dichloromethane solution at −50 °C one equivalent of oxalyl chloride gave the 6-carbaldehyde derivative. ^1H NMR spectra of the greasy solids obtained directly after removal of all volatiles from the two reaction mixtures showed that the derivatives were formed in near quantitative yield. The synthesis of the 6-chloromethyl derivative is akin to that of the 5-chloromethyl derivative reported by Karlin and co-workers.[7] EI mass spectra of both derivatives exhibit intense peaks for the molecular ions and a strong ν_{CO} peak at 1710 cm^{-1} is seen in the FTIR spectrum of the 6-carbaldehyde. Chromatography of the 6-chloromethyl derivative afforded an analytical quality sample with the same spectroscopic properties as the crude product. The aldehyde derivative was unstable to chromatography and an analytical quality sample was not obtained. We expect that H_2L^2 and H_3L^3 should react similarly and we are currently attempting to prepare multi-nucleating and cofactor-substituted ligands built around the tpa core starting from these chloromethyl or carboxaldehyde derivatives.

Copper(II) complexes. The co-ordination chemistry of HL^1, H_2L^2 and H_3L^3 with copper(II) chloride and copper(II) tetrafluoroborate was investigated. Unless anhydrous conditions were employed, reactions of HL^1, H_2L^2 and H_3L^3·*x*NaBr with copper(II) chloride produced blue oils that could not be induced to crystallise. This probably reflects the ability of the complexes that form tenaciously to retain traces of water or solvent through hydrogen bonding interactions with the hydroxymethyl group(s). However, using anhydrous conditions the crystalline (chloro)copper(II) complexes $[Cu(HL^1)Cl]Cl$ **1**, $[Cu(H_2L^2)Cl]Cl$ **2** and, following metathesis of **2** with sodium *p*-toluenesulfonate [Na(OTs)], $[Cu(H_2L^2)Cl][OTs]$ **3** were obtained.

Reaction of H_2L^2 and copper tetrafluoroborate in dry acetonitrile produced a surprise. Resplendent blue crystals of $[Cu(L^2BF_2)][BF_4]$ **4** deposited in ≈30% yield directly from the reaction mixture when it was set aside under an atmosphere of diethyl ether. The borate ester linkages in the new macrocyclic ligand, $L^2BF_2^-$, most likely form by copper(II)-templated nucleophilic attack of the hydroxymethyl groups on a tetrafluoroborate anion. The $(RCH_2O)_2BF_2^-$ donor group is new. Whereas linking two oximato groups to give borate ester-linked macrocyclic ligands is well known,[19] we are unaware of any transition metal complexes with a $(RCH_2O)_2BF_2^-$ *O*-donor group. Moreover, although Lehn and co-workers have reported cryptands incorporating the tpa core,[20] to our knowledge this is the first example of a macrocyclic ligand obtained by linking together two arms of the tpa core.

The reactions of H_3L^3·*x*NaBr with copper(II) salts were more complicated. Before it was recognised that H_3L^3 was always obtained as a mixture with sodium bromide, the mixture H_3L^3·*x*NaBr was added to copper(II) chloride in methanol to produce a green solution which turned brown on standing for several hours. A brown greasy solid formed over several days. Recrystallisation of this solid from anhydrous tetrahydrofuran gave a mixture of green and brown crystals. The brown crystals have been crystallographically determined to be $[Cu(H_3L^3)Br_{0.43}Cl_{0.57}]_2[Cu(Br_{0.43}Cl_{0.57})_2(Br_{0.97}Cl_{0.03})_2]$ **5** with compositionally disordered bromo and chloro co-ligands (see below). Unfortunately, the green crystals were not of sufficient quality for X-ray crystallographic analysis and their identity remains unknown. Using copper(II) bromide with H_3L^3·*x*NaBr under similar conditions afforded $[Cu(H_3L^3)Br]Br$ **6**. The reaction of H_3L^3·*x*NaBr with copper(II) tetrafluoroborate in dry methanol followed a different course. The reaction mixture turned green and a purple sticky solid formed when it was placed under a diethyl ether atmosphere for several days. This was recrystallised from anhydrous 4:1 butanol–tetrahydrofuran to produce a few green crystals of the novel trimer $[Cu_3\{H_3(L^3)_2\}Br][BF_4]_2$ **7**.

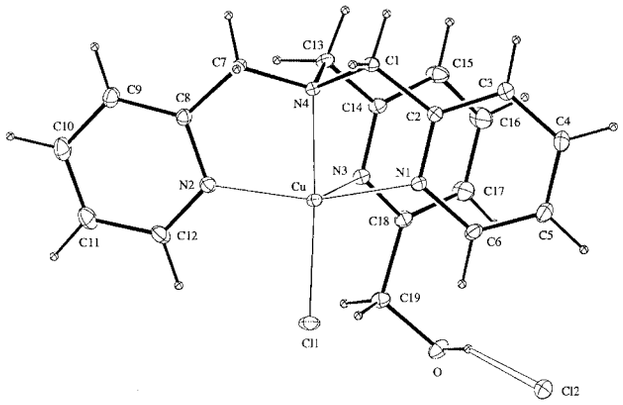

Fig. 1 View of $[Cu(HL^1)Cl]Cl$ **1** (10% thermal ellipsoids at 294 K in all views).

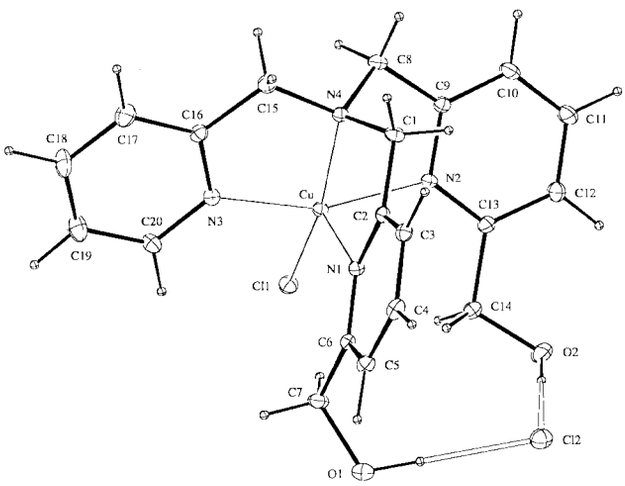

Fig. 2 View of $[Cu(H_2L^2)Cl]Cl$ **2**.

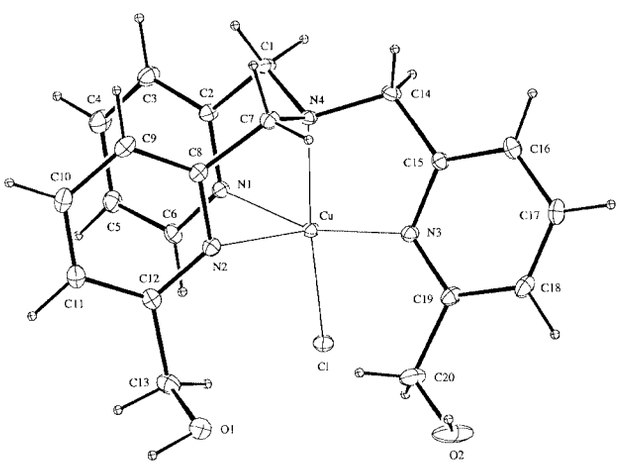

Fig. 3 View of the cation from the crystal structure of $[Cu(H_2L^2)Cl][OTs]$ **3**.

Crystal structures

All seven copper(II) complexes, **1**–**7**, have been characterised by X-ray crystallography.

$[Cu(HL^1)Cl]Cl$ 1, $[Cu(H_2L^2)Cl]X$ (X = Cl 2 or OTs 3). Figs. 1–3 illustrate the structures of the cations in complexes **1**–**3**, and relevant bond distance and angle data are given in Table 1. Each cation is five-co-ordinate and analysis gives τ trigonality indices of 0.14 for **1**, 0.03 for **2** and 0.10 for **3**. Thus the stereochemistry about the copper(II) ion in each cation is close to square pyramidal [$\tau = (\alpha - \beta)/60$ where α and β are the largest and next largest bond angles about the central copper ion; τ is 0 for a perfect square pyramid and 1.0 for a perfect trigonal bipyramid[21]]. In each complex cation, the weak-field, axial co-ordination site is taken up by a hydroxymethylpyridyl (py*) group thereby minimising the steric interactions of this group with the basal donor groups which are chloride and the amine and two remaining pyridyl groups. As expected, the Cu–N(py*) apical bond distances of 2.472(2) Å in **1**, 2.253(3) Å in **2** and 2.395(2) Å in **3** are significantly longer than the average basal Cu–N(py/py*) bond distances of 2.015 Å in **1** and 2.036 Å in **2** and **3**. The apical pyridyl rings are significantly bent away from the Cu–N(py*) vectors by 40.0° in **1**, by 12.4° in **2** and by 35.6° in **3**, *e.g.* Fig. 4(a). The different angles for **2** and **3**, which contain the $[Cu(H_2L^2)Cl]^+$ cation, suggest that to some extent at least the positioning of the axial hydroxymethylpyridyl group is dictated by crystal packing. Unexceptional Cu–Cl and Cu–N(amine) distances are observed, Table 1.

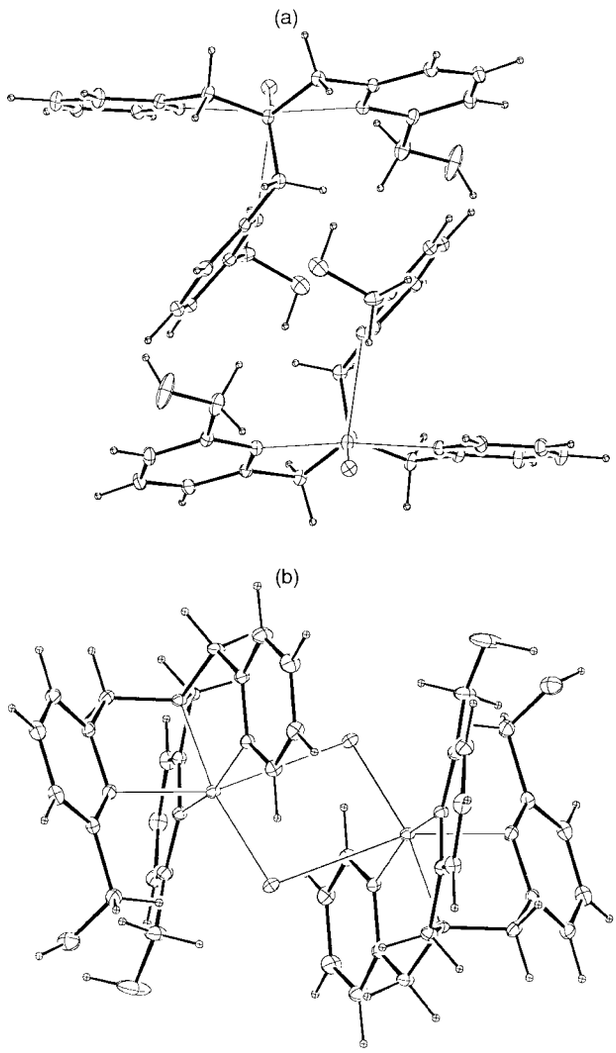

Fig. 4 The two pairings of $[Cu(H_2L^2)Cl]^+$ ions in the crystal structure of $[Cu(H_2L^2)Cl][OTs]$ **3**. (a) View of pair with π-stacked axial hydroxymethylpyridyl rings, emphasising the tilt of these rings away from the Cu–N vector (see text). (b) View of pair revealing the semi-bridging nature of the chloro co-ligands. The long Cu · · · Cl distance is 3.142 Å.

The crystal structures of complexes **1**–**3** differ. In **1** there are no close intercation contacts (the closest not involving a hydrogen atom is ≈4.6 Å between the nitrogens of the axial pyridyl groups of neighbouring cations). The hydroxymethyl group of each cation is hydrogen bonded with a chloride ion (O · · · Cl2 3.120 Å), Fig. 1. Likewise, in the crystal structure of **2** the two hydroxymethyl groups of each cation hydrogen bond to a single chloride ion (O2 · · · Cl2 3.094, O1 · · · Cl2 3.139 Å), Fig. 2. Cations of **2** pack with four antiparallel neighbours, and with

Table 1 Selected bond lengths (Å), bond angles (°) and trigonality (τ) parameters for complexes **1**, **2** and **3**

1		**2**		**3**	
Cu–Cl1	2.234(1)	Cu–Cl1	2.247(1)	Cu–Cl	2.262(1)
Cu–N2	1.999(2)	Cu–N1	2.253(3)	Cu–N1	2.018(2)
Cu–N3	2.472(2)	Cu–N2	2.051(3)	Cu–N2	2.395(2)
Cu–N1	2.008(2)	Cu–N3	2.000(4)	Cu–N3	2.052(2)
Cu–N4	2.037(2)	Cu–N4	2.057(3)	Cu–N4	2.038(2)
Cl1–Cu–N2	97.3(1)	Cl1–Cu–N1	118.1(1)	Cl–Cu–N1	93.4(1)
Cl1–Cu–N3	107.6(1)	Cl1–Cu–N2	97.1(1)	Cl–Cu–N2	109.8(1)
Cl1–Cu–N1	98.7(1)	Cl1–Cu–N3	94.9(1)	Cl–Cu–N3	101.2(1)
Cl1–Cu–N4	171.4(1)	Cl1–Cu–N4	161.5(1)	Cl–Cu–N4	168.3(1)
N2–Cu–N3	98.2(1)	N1–Cu–N2	96.9(1)	N1–Cu–N2	84.6(1)
N2–Cu–N1	162.9(1)	N1–Cu–N3	92.0(1)	N1–Cu–N3	162.1(1)
N2–Cu–N4	81.0(1)	N1–Cu–N4	80.4(1)	N1–Cu–N4	82.8(1)
N3–Cu–N1	82.7(1)	N2–Cu–N3	159.5(1)	N2–Cu–N3	99.8(1)
N3–Cu–N4	81.0(1)	N2–Cu–N4	80.0(1)	N2–Cu–N4	81.1(1)
N1–Cu–N4	82.2(1)	N3–Cu–N4	83.3(1)	N3–Cu–N4	80.8(1)
τ	0.14		0.03		0.10

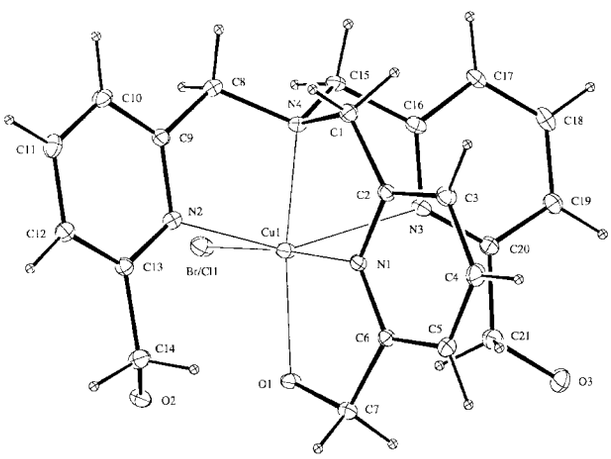

Fig. 5 View of the $[Cu(H_3L^3)Br_{0.43}Cl_{0.57}]^+$ ion from the crystal structure of complex **5**.

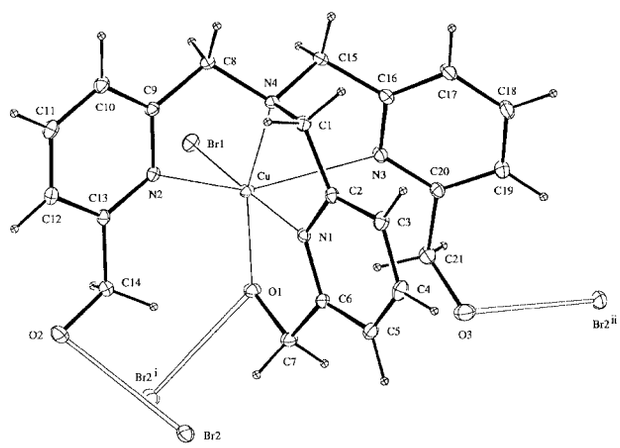

Fig. 6 View of $[Cu(H_3L^3)Br]Br$ **6**. Symmetry positions are: i $-x$, $1-y$, $-z$; ii $\frac{1}{2}-x$, $\frac{1}{2}+y$, z.

each pyridyl ring of the cations involved in edge-to-face interactions (the edge carbon-to-adjacent ring plane distances are ≈3.60–3.75 Å) with a pyridyl ring of an adjacent cation. Fig. 4(a) shows pairs of adjacent complex cations, related by crystallographic inversion, in the crystal structure of **3**. The axial pyridyl groups of each cation in the pair π-stack at a typical distance of 3.5–3.6 Å. Fig. 4(a) also illustrates the bending of each axial pyridyl group away from its Cu–N vector (a common feature in the structures of **1**–**3**, see above). This compresses the distance between the cations such that the remaining space is taken up neatly by the tosylate anions which hydrogen-bond with the hydroxymethyl groups. A second structural motif found in the crystal structure of **3** is that each cation also pairs with a second adjacent cation such that the chloro ligand of each cation in this pair occupies the sixth octahedral position of the other, Fig. 4(b). The Cu···Cl distance is 3.142 Å and, although too long to be a bond, it presumably stabilises the crystal structure. This structural motif is also found in the crystal structure of **2**, but the pairs are more separated at a much longer Cu···Cl distance of 3.763 Å.

$[Cu(H_3L^3)(Br/Cl)]_2[Cu(Br/Cl)_4]$ 5 and $[Cu(H_3L^3)Br]Br$ 6. As already noted complex **5** has compositionally disordered bromide and chloride ligands. Both complexes contain a $[Cu(H_3L^3)X]^+$ (refines to $X = Br_{0.43}Cl_{0.57}$ **5** or Br **6**) cation with similar overall structure, Figs. 5 and 6. The counter ion in **5** is the $[Cu(Br_{0.43}Cl_{0.57})_2(Br_{0.97}Cl_{0.03})_2]^{2-}$ anion, which has an axially compressed tetrahedral geometry[22] and refines with different bromide and chloride occupancies for the two independent halide sites (see electronic supplementary information, Fig. 1). The Br/Cl–Cu–Br/Cl angles in the anion are two of 129.4(1)°, two of 99.7(1), 104.5(1) and 97.9(1)°. In the crystal structure of **5** pairs of adjacent cations related by a crystallographic inversion centre are hydrogen bonded with O2···O3′ (adjacent cation) 3.188 Å. Bromide ion is the counter anion in **6**, and in the crystal structure each bromide ion forms hydrogen bonds to a different hydroxymethyl group in each of three neighbouring cations with Br2···O1 3.163, Br2···O2′ (second adjacent cation) 3.260 and Br2···O3″ (third adjacent cation) 3.382 Å.

Selected bond angles and distances for complexes **5** and **6** are given in Table 2. In both cations the copper(II) ion is bound by the amine, all three pyridyl nitrogens and one oxygen of the hydroxymethylpyridyl arms of ligand H_3L^3. The *N*,*O*-co-ordinated arm of the ligand lies in the equatorial plane of a tetragonally elongated octahedron at normal bond distances [**5**: Cu–N1 1.921(4), Cu–O1 2.070(3) Å. **6**: Cu–N1 1.944(3), Cu–O1: 2.065(2) Å]. The two other equatorial positions are taken by the halogen ligand [in **6** Cu–Br1 is 2.362(1) Å], *trans* to the equatorial pyridyl nitrogen, and by the amino nitrogen [Cu–N4: 2.066(4) Å in **5** and 2.092(3) Å in **6**], *trans* to the hydroxymethyl oxygen. The shift in the halogen ligand to *trans* to the equatorial pyridyl, compared to *trans* to the amine group in **1**–**3**, is required for co-ordination of the hydroxymethyl OH group. Long, and presumably, weak Cu–N bonds are observed to the two transoid hydroxylmethylpyridyls in the weak-field, axial positions of the elongated octahedra [**5**: Cu–N2 2.429(4) and Cu–N3 2.556(4) Å. **6**: 2.322(3) and 2.782(3) Å]. The tetragonality parameter (T)[22] for **5** is 0.84 and for **6** is 0.83,

Table 2 Selected bond lengths (Å) and bond angles (°) for complexes **5** and **6**

5		**6**	
Cu1–Br/Cl1	2.314(1)	Cu–Br1	2.362(1)
Cu1–O1	2.070(3)	Cu–O1	2.065(2)
Cu1–N1	1.921(4)	Cu–N1	1.944(3)
Cu1–N2	2.429(4)	Cu–N2	2.322(2)
Cu1–N3	2.556(4)	Cu–N3	2.782(3)
Cu1–N4	2.066(4)	Cu–N4	2.092(3)
Br/Cl1–Cu1–O1	95.8(1)	Br1–Cu–O1	96.3(1)
Br/Cl1–Cu1–N1	175.1(1)	Br1–Cu–N1	170.4(1)
Br/Cl1–Cu1–N2	94.7(1)	Br1–Cu–N2	93.9(1)
Br/Cl1–Cu1–N3	97.2(1)	Br1–Cu–N3	97.4(1)
Br/Cl1–Cu1–N4	99.6(1)	Br1–Cu–N4	100.6(1)
O1–Cu1–N1	80.1(1)	O1–Cu–N1	78.4(1)
O1–Cu1–N2	101.2(1)	O1–Cu–N2	113.1(1)
O1–Cu1–N3	104.5(1)	O1–Cu–N3	95.4(1)
O1–Cu1–N4	164.5(1)	O1–Cu–N4	160.2(1)
N1–Cu1–N2	88.8(1)	N1–Cu–N2	95.6(1)
N1–Cu1–N3	81.4(1)	N1–Cu–N3	75.4(1)
N1–Cu1–N4	84.6(1)	N1–Cu–N4	83.3(1)
N2–Cu1–N3	150.2(1)	N2–Cu–N3	147.9(1)
N2–Cu1–N4	76.5(1)	N2–Cu–N4	76.1(1)
N3–Cu1–N4	74.7(1)	N3–Cu–N4	72.3(1)

Table 3 Selected bond lengths (Å) and bond angles (°) for complex **4**

Cu–N1	2.189(4)	O1–B	1.494(7)
Cu–N2	1.931(4)	O2–C20	1.383(6)
Cu–N3	1.981(4)	O2–B	1.428(7)
Cu–N4	2.041(4)	B–F1	1.388(6)
Cu–O1	1.966(3)	B–F2	1.379(7)
O1–Cl3	1.423(6)		
O1–Cu–N1	105.8(1)	N1–Cu–N3	114.9(2)
O1–Cu–N2	80.5(2)	N1–Cu–N4	81.1(2)
O1–Cu–N3	105.8(2)	N2–Cu–N3	143.9(2)
O1–Cu–N4	163.2(1)	N2–Cu–N4	83.4(2)
N1–Cu–N2	96.5(2)	N3–Cu–N4	72.3(1)

consistent with thermally invariant (static) tetragonally elongated structures for both cations. The asymmetry in the axial Cu–N bond lengths suggests that **6** is bordering on square pyramidal co-ordination. Also noteworthy in the structure of **5** is the intra-cation hydrogen bond between the OH group of the equatorial hydroxymethylpyridyl arm and the closer axial hydroxymethylpyridyl arm (O1 · · · O2 2.609 Å).

[Cu(L^{2}BF$_2$)][BF$_4$] 4. Immediately apparent from the structure of complex **4** is that a copper(II) ion-assisted reaction of H_2L^2 and $[BF_4]^-$ ion has linked the two hydroxymethylpyridyl "arms" together thereby forming the novel, macrocyclic borate ester ligand $L^2BF_2^-$, Fig. 7. The copper(II) ion in **4** exhibits trigonally distorted square pyramidal co-ordination ($\tau = 0.32$). Whereas the structures of **1**–**3** and **5** and **6** reveal weak-field, axial positioning for at least one of the hydroxymethyl-substituted pyridyl rings, formation of the macrocyclic ring constrains the nitrogen donor atoms of the 2,6-substituted pyridyl rings (*i.e.*, N2 and N3) to the square base which is completed by the amine nitrogen (N4) and one of the ester oxygen (O1) atoms. The bond distances from these basal donor atoms to the copper(II) ion are unexceptional, Table 3. The remaining pyridine nitrogen occupies the apical position of the square pyramid 2.189(4) Å away from the copper(II) ion. The second ester group is too far from the copper(II) ion [Cu · · · O2 2.811(5) Å] to be considered co-ordinated to it.

[Cu$_3${H$_3$(L^3)$_2$}Br][BF$_4$]$_2$ 7. Fig. 8 gives two views of the trimeric dication, **7**, which displays approximate C_2 symmetry. The cation is comprised of a central, BrN_2O_2-co-ordinated copper ion (Cu) and two outer, N_3O_2-co-ordinated copper ions

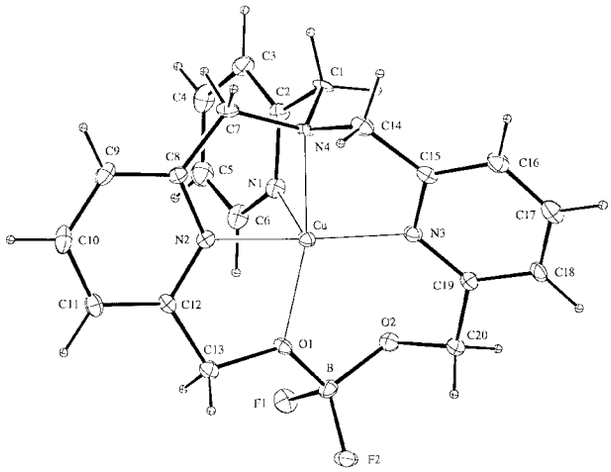

Fig. 7 View of the cation of [Cu(L^{2}BF$_2$)][BF$_4$] **4**.

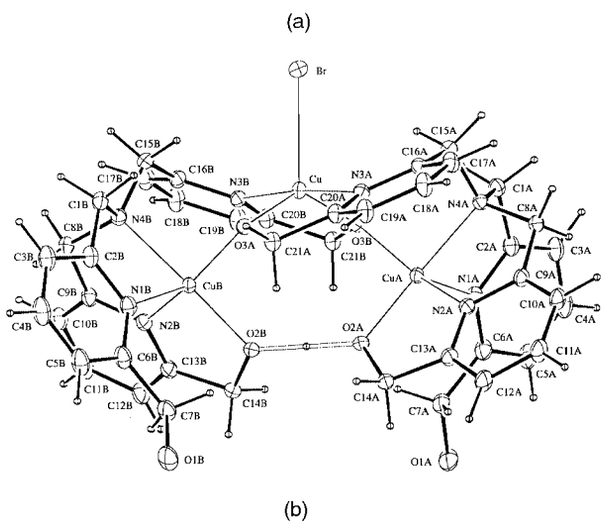

Fig. 8 Views from the crystal structure of [Cu$_3${H$_3$(L^3)$_2$}Br][BF$_4$]$_2$·0.5 C$_4$H$_9$OH·thf **7** of the trimeric cation approximately perpendicular (a) and parallel (b) to the pseudo-twofold axis; the H atoms are removed for clarity in (b).

(CuA and CuB). The copper ions are bridged by the two organic ligands, with each hydroxymethylpyridyl (pyridylmethanol) arm of these ligands having a different role. The amine and two arms of each organic ligand are bonded to an outer copper, one arm by the pyridyl group only and the other by both the pyridyl and the methanol(ate) groups. Of the latter methanol groups, one is deprotonated and forms a strong, symmetric hydrogen bond with the other [O–H · · · O: O2A · · · O2B 2.372 Å], closing the base of the triangular

Table 4 Selected bond lengths (Å), bond angles (°) and trigonality (τ) parameters for complex **7**

Cu		CuA		CuB	
O3B–Cu	1.955(7)	CuA–O2A	1.976(6)	CuB–O2B	1.984(7)
N3A–Cu	2.053(5)	CuA–N1A	2.220(5)	CuB–N1B	2.252(6)
O3A–Cu	1.950(6)	CuA–N2A	1.889(5)	CuB–N2B	1.892(5)
N3B–Cu	2.055(5)	CuA–N4A	2.082(8)	CuB–N4B	2.101(8)
Cu–Br	2.603(2)	CuA–O3B	1.907(6)	CuB–O3A	1.914(6)
03A–Cu–N3A	82.6(3)	O2A–CuA–N1A	116.2(3)	O3A–CuB–O2B	98.4(3)
O3A–Cu–O3B	134.0(3)	O2A–CuA–N2A	82.0(3)	O3A–CuB–N1B	97.5(3)
O3A–Cu–N3B	95.6(3)	O2A–CuA–N4A	159.8(3)	O3A–CuB–N2B	156.5(3)
O3A–Cu–Br	116.0(2)	O2A–CuA–O3B	99.0(3)	03A–CuB–N4B	91.2(3)
N3A–Cu–O3B	94.6(3)	N1A–CuA–N2A	102.1(3)	O2B–CuB–N1B	116.4(3)
N3A–Cu–N3B	173.7(3)	N1A–CuA–N4A	79.4(3)	O2B–CuB–N2B	82.3(3)
N3A–Cu–Br	93.8(2)	N1A–CuA–O3B	96.1(3)	O2B–CuB–N4B	161.1(3)
O3B–Cu–N3B	82.3(3)	N2A–CuA–N4A	82.2(3)	N1B–CuB–N2B	103.2(3)
O3B–Cu–Br	110.1(2)	N2A–CuA–O3B	159.2(3)	N1B–CuB–N4B	78.1(3)
N3B–Cu–Br	92.4(2)	N4A–CuA–O3B	91.5(3)	N2B–CuB–N4B	82.5(3)
τ	0.66		0.01		0.08

copper cluster, Fig. 8(a). The third, pyridylmethanolate arm bridges the other two copper ions, with the pyridyl co-ordinated to the central copper and the (deprotonated) methanolate group bridging between the central and other outer copper ion, Fig. 8(b). One of the two hydroxymethyl groups not bonded to copper forms a hydrogen bond with the bromine of the adjacent trimer [O1A · · · Br′ 3.228 Å]. The other (O1B) is directed towards the disordered lattice molecules of butanol and thf. There are no other significant intermolecular interactions in the crystal structure.

The two outer copper ions, CuA and CuB, are square-pyramidal (τ values are 0.01 and 0.08) with the basal plane made up by the amine and the pyridyl and methanol(ate) groups of the N,O-co-ordinated arm of one organic ligand, and by the O-methanolate oxygen of the bridging arm of the other organic ligand. Bond distances from these donors to the copper ions are unexceptional, Table 4. Each N-co-ordinated hydroxymethylpyridyl arm adopts the axial position of the square-based pyramid with CuA–N1A 2.220(5) Å and CuB–N1B 2.252(6) Å. The central copper ion, Cu, is bonded by the pyridyl nitrogen [N3(A,B)] and the methanolate oxygen [O3(A,B)] of the bridging arm of each ligand at typical distances, Table 4, and by a bromide ligand; the Cu–Br bond distance at 2.603(2) Å is long and suggestive of bonding along a weak-field axis. However, with a τ value of 0.66, the geometry about the central copper ion is best described as intermediate between square pyramidal (with an axial bromide) and trigonal bipyramidal [with axial pyridyls: N3A–Cu–N3B 173.7(3)° compares with O3A–Cu–O3B 134.0(3)°]. The inter-copper distances in the trimer are Cu · · · CuA 3.148, Cu · · · CuB 3.157 and CuA · · · CuB 4.981 Å. An obvious comparison to make is with the tricopper centres in multicopper oxidases such as ascorbate oxidase, laccase and ceruloplasmin.[15] These proteins couple oxidation of their substrate(s) to four-electron reduction of dioxygen at a tricopper active site which has a common structure. For the tricopper cluster of ascorbate oxidase the inter-copper distances are 3.66, 3.7 and 3.78 Å in its fully oxidised [all copper(II)] form and 3.7, 4.5 and 4.8 Å in its peroxide-bound [all copper(II)] form.[15]

Characterisation and physicochemical properties

Correct elemental analyses were obtained for complexes **1**–**4** and **6**. Elemental analyses of **5** (Br/Cl compositionally disordered) and **7** (too small a sample) were not obtained and the formulae given for these compounds are based on the crystal structure analyses described above and on the following spectroscopic data. Electrospray ionisation (ES) mass spectra of **1** exhibit intense peaks corresponding to fragment ions

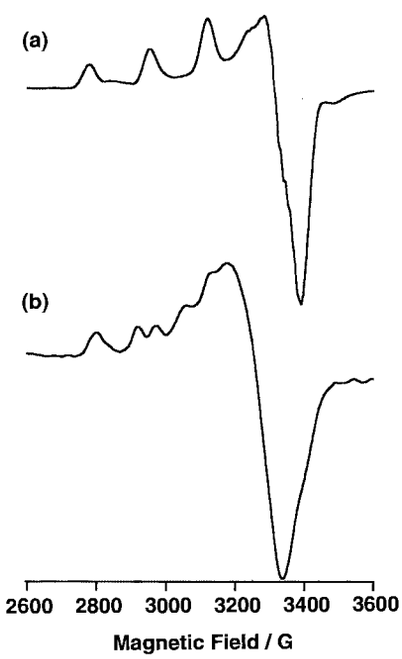

Fig. 9 X-Band EPR spectra of $[Cu(H_2L^2)Cl]Cl$ **2** (a) and $[Cu_3\{H_3(L^3)_2\}Br][BF_4]_2$ **7** (b): methanol glass, 77 K, ν/GHz = 9.502.

$[Cu(HL^1)Cl]^+$ (*m*/*z* 420) and $[Cu(HL^1)]^+$ (*m*/*z* 382), whilst the ES mass spectrum of **2** shows peaks for the ions $[Cu(H_2L^2)(OAc) + H]^+$ (*m*/*z* 470) arising from acetate for chloride exchange [the feed solvent in the ES MS experiments was 1% acetic acid (HOAc) in 1 : 1 v/v acetonitrile–water], $[Cu(H_2L^2)Cl]^+$ (*m*/*z* 448) and $[Cu(H_2L^2)]^+$ (*m*/*z* 412). The ES mass spectrum of **3** reveals peaks at *m*/*z* 639, 448 and 412 corresponding to the ions $[Cu(H_2L^2)Cl + OTs]^+$, $[Cu(H_2L^2)Cl + H]^+$ and $[Cu(H_2L^2)]^+$, respectively. Complexes **5** and **6** display simple ES mass spectra with two intense isotopic peaks at *m*/*z* 444 and 222 for the ions $[Cu(H_3L^3)]^+$ and $[Cu(H_3L^3)]^{2+}$. The ES mass spectrum of complex **7** also shows these peaks and, most notably, a peak at *m*/*z* 515 for the parent molecular ion, $[Cu_3\{H_3(L^3)_2\}Br]^{2+}$. This provides some evidence for the structure found in the crystal structure of **7** persisting in solution and into the gas phase.

EPR spectra of complexes **1**–**4** and **6**, recorded in frozen methanol glasses at 77 K, are axial (*e.g.*, Fig. 9a) and consistent with tetragonally elongated octahedral or square pyramidal structures ($d_{x^2-y^2}$ ground states).[12,13,22,23] Vis/NIR spectra of **1**–**6** in methanol solution show broad bands having maxima at ≈715–725 nm and prominent shoulders or tails to lower energy

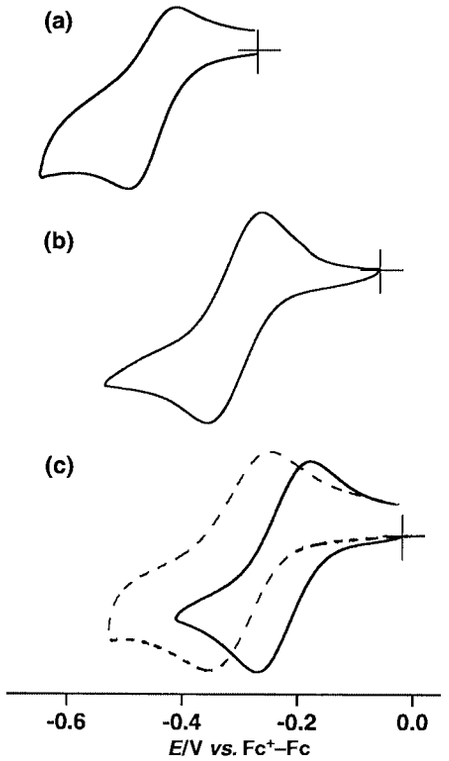

Fig. 10 Cyclic voltammograms of complex **1** (a), **2** (b), **5** (c: – – –) and **6** (c: ——) in acetonitrile solution. Conditions: freshly polished platinum disc electrode, scan rate = 100 mV s^{-1}, temperature = 296 K.

(see electronic supplementary information, Fig. 2), consistent with each complex adopting a very distorted square pyramidal structure in solution.[12,13,22,23] For comparison, the square pyramidal [Cu(tepa)Cl]$^+$ [tepa = tris(2-pyridylethyl)amine] ion in MeCN solution shows a band at 665 (ε 200) with a prominent shoulder at 967 nm (ε 48 M^{-1} cm^{-1}). In sum, the data point to **1**–**6** having distorted square pyramidal structures in solution. UV/Vis/NIR spectra were also obtained for crystalline **1**, **2**, and **6** dispersed in KBr discs. For **1** and **2** the spectra were very similar to those found in methanol solution with each complex exhibiting a broad band (at 722 nm for **1** and 695 nm for **2**) with a distinct tail to low energy. The spectrum of a KBr disc containing **6** showed only a broad tail in the visible region extending from the intense charge transfer band at ≈280 nm. The EPR spectrum of **7**, Fig. 9(b), is more complicated than the simple axial spectra seen for **1**–**4** and **6**, and is consistent with more than one copper centre as expected. There is no evidence for a half-field transition. A simple first-order simulation (with neglect of dipolar coupling) as two overlapping axial subspectra is satisfactory and suggests the following parameters for the two types of copper centre: $g_{\|} = 2.27$, $A_{\|} = 126$ G, $g_{\perp} \approx 2.03$ for one copper and $g_{\|} = 2.18$, $A_{\|} = 150$ G, $g_{\perp} \approx 2.07$ for two coppers. The Vis/NIR spectra of **7** in methanol solution and in the solid-state are very similar (electronic supplementary information, Fig. 3), displaying an intense band at 260 nm and a broad, asymmetric visible band at 703 nm with a distinct tail to low energy, indicative of **7** retaining its structure in solution. Since only several small crystals were available, a more detailed study of the physicochemical properties of complex **7** was not undertaken.

Cyclic voltammograms of complexes **1**–**6** in acetonitrile–0.1 M [Bu^n_4N][PF_6] display quasireversible Cu^{II}–Cu^{I} couples ($\Delta E_p \approx 90$–120 mV compared to 75 mV for the Fc^+–Fc couple), Fig. 10. Peak current ratios were near unity except for **1** ($i_{pc}/i_{pa} \approx 0.3$) and **6** ($i_{pc}/i_{pa} \approx 0.6$) (Table 5). The potentials ($E_{1/2}$) shift positive in the order **1** < **2** ≈ **3** ≈ **6** < **5**. Each increase in 6-hydroxymethyl substitution of the pyridyls along the series [Cu(tpa)Cl]$^+$,[13] **1**, **2** and **5** stabilises the copper(I) complex by

Table 5 Data (in volts *vs.* ferrocenium–ferrocene) from cyclic voltammograms (scan rate = 100 mV s^{-1}) of complexes (1 mM) in acetonitrile–0.1 M tetrabutylammonium hexafluorophosphate at 25 °C

Complex	$E_{1/2}$/V	ΔE_p/mV	i_{pa}/i_{pc}
[Cu(tpa)Cl]$^+$ [a]	−0.69		
1	−0.51	120	0.28
2	−0.36	100	0.80
4	−0.405	150	0.95
5	−0.225	90	0.80
6	−0.315	95	0.60
7	−0.27	130	0.90
	−0.59 (E_{pc})		

[a] Reference 13.

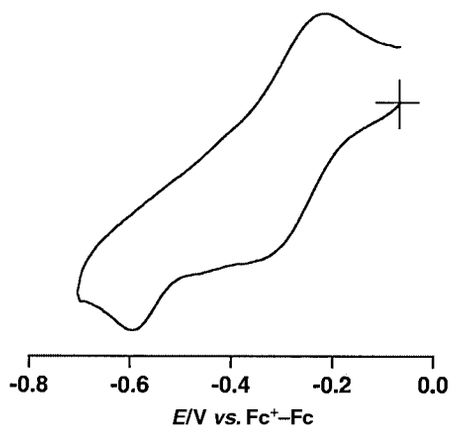

Fig. 11 Cyclic voltammogram of complex **7**; conditions as for Fig. 10.

≈140–180 mV. Other studies also reveal that the Cu^{II}–Cu^{I} couples for copper complexes of tpa derivatives also move increasingly positive with more 6-substitution. For example, Nagao *et al.* report that the redox potentials of the [Cu(H_2O){(6-Me)$_n$tpa}]$^{2+}$ (n = 0, 1, 2 or 3) series in acetonitrile or water increase in the order of tpa < Metpa < Me_2tpa < Me_3tpa.[12] Likewise, Chuang *et al.* report that each 6-phenyl group in the [Cu(Ph_ntpa)(MeCN)]$^{2+}$ (n = 0, 1, 2 or 3) series contributes ≈+100 mV towards the Cu^{II}–Cu^{I} couple.[11] Increasing 6-substitution of the pyridyl rings in tpa derivatives clearly destabilises the copper(II) complex relative to the copper(I) complex. Exactly why remains unclear. To explain this trend for the [Cu(Ph_ntpa)(MeCN)]$^{2+}$ (n = 0, 1, 2 or 3) series, Chuang *et al.* have advanced arguments based on the non-polar 6-phenyl substituents occluding the metal ion from the solvent dielectric and thereby favouring the lower oxidation state, copper(I).[10,11] However, the same trend is found with polar 6-hydroxymethyl substituents and, accordingly, we favour increasing steric interactions destabilising the copper(II) complex as the underlying reason for the positive shift in the Cu^{II}–Cu^{I} couple with increasing 6-substitution of the tpa-core. Indeed this is consistent with the recent conclusions by Rorabacher and colleagues that Cu^{II}–Cu^{I} couples are most influenced by the stabilities of the copper(II) state, with the copper(I) state exerting little effect.[24] We have recently estimated that if a copper(I) complex displays a Cu^{II}–Cu^{I} couple in acetonitrile negative of ≈0 V *vs.* Fc^+–Fc then it should react with dioxygen.[25] Therefore, we predict that copper(I) complexes of HL^1, H_2L^2 and H_3L^3 should form adducts with dioxygen, perhaps by hydrogen bonding between the superoxo or peroxo ligand and the hydroxymethyl group(s).[6] Studies of the copper(I) complexes are under way.

Cyclic voltammograms of complex **7** reveal a quasi-reversible reduction at −0.27 V followed by a second, irreversible reduction at −0.59 V with a peak current half that for the first process, Fig. 11. As mentioned above, electrospray mass, EPR and electronic spectra point to **7** retaining its trimeric structure

in solution. Each copper ion in the trimer should be redox-active and exhibit a Cu^{II}–Cu^{I} couple. A possible assignment based on peak currents is that the quasi-reversible reduction process at −0.27 V results from the simultaneous one-electron reduction of each of the two outer copper(II) ions, consistent with these acting as independent non-interacting copper centres, and that the irreversible process at −0.59 V arises from reduction of the central copper(II) ion. Loss of bromide ion is anticipated upon reduction of the central copper(II) ion, and possibly could account for the irreversible nature of the reduction. There was insufficient sample of **7** for further (spectro)electrochemical experiments to confirm these preliminary assignments.

In conclusion, we have successfully developed a practicable route to tpa derivatives functionalised at the 6 position by hydroxymethyl, chloromethyl or carbaldehyde groups on the pyridine rings. These should prove useful precursors to multi-nucleating and cofactor-substituted ligands based on the tpa unit. It is shown that the 6-hydroxymethyl-substituted tpa ligands are in themselves interesting, the copper(II) co-ordination chemistry being particularly fertile. We anticipate equally rich chemistries with other transition metals and with the lanthanide and actinide elements.

Experimental

Physical measurements

^{1}H NMR spectra were recorded on a Bruker AC 300F (300 MHz) spectrometer and EPR spectra on a Bruker EMX 10 EPR spectrometer. Quoted EPR data are from simulations of the experimental spectrum.[26] Mass spectra were acquired on a VG Quattro mass spectrometer. For EI mass spectra, a 70 eV ionising potential and an ion source temperature of 210 °C was used. For ES mass spectra, a capillary voltage of 4 kV and a cone voltage of 30 V were utilised at 60 °C, and the feed solvent was 1% acetic acid in 1:1 v/v acetonitrile–water. Elemental analyses for C, H and N were determined by the Microanalysis Unit, Research School of Chemistry, Australian National University. Prior to analysis, samples were dried at 40 °C for 24 h under vacuum (0.2 mmHg) over phosphorus pentaoxide. Infrared spectra were recorded on KBr discs using a Mattson Genesis Series FTIR spectrometer, electronic spectra on a CARY 5 spectrometer in the dual beam mode using quartz cells (1 cm) with methanol as the solvent. Cyclic voltammograms were recorded at freshly polished Pt-disc working electrodes using a Pine Instrument Co. AFCBP1 Bipotentiostat interfaced to and controlled by a Pentium computer. Data are referenced relative to the ferrocenium–ferrocene (Fc^+–Fc) couple which was measured *in situ* as an internal standard. Full experimental details for the electrochemical experiments are published elsewhere.[25,27]

Materials and reagents

Reagents were obtained from commercial suppliers and used without further purification. The following solvents were distilled from the appropriate drying agent under a dinitrogen atmosphere immediately prior to use: toluene from CaH_2, ethanol from magnesium ethoxide formed from magnesium turnings activated with iodine, THF and diethyl ether from sodium–benzophenone, acetonitrile from CaH_2, and chloroform and dichloromethane from P_2O_5. Flash chromatography was carried out using Merck silica gel 7730 $60GF_{254}$.

Preparations

[6-(Hydroxymethyl)-2-pyridylmethyl]bis(2-pyridylmethyl)-amine, HL[1]. A solution of *N*,*N*-bis(2-pyridylmethyl)amine (2.220 g, 11.1 mmol) and triethylamine (1.55 mL, 11.1 mmol) in acetonitrile (40 mL) was added dropwise over 2 h to a solution of 6-(bromomethyl)-2-(hydroxymethyl)pyridine[17] (2.24 g, 11.1 mmol) in acetonitrile (30 mL). The yellow reaction mixture was stirred for 18 h under a dinitrogen atmosphere, over which time it became dark orange. Completion of the reaction was monitored by thin layer chromatography, which showed that the reaction mixture only contained one compound that was neither of the two starting materials. Evaporation of acetonitrile on the rotary evaporator yielded a brown oil. Chloroform was added to the oil and the organic phase washed with saturated $NaHCO_3$ and brine solutions. The organic phase was dried over anhydrous magnesium sulfate, and the solvent evaporated to give a clear yellow oil (3.40 g, 95%). EI-MS: *m*/*z* 641 (M_2H^+, 2%), 321 (MH^+, 12) and 200 ($M - CH_2C_5H_3NCH_2OH^+$, 100). λ_{max}/nm(CH_3CN) 265 (ε/dm^3 mol^{-1} cm^{-1} 9420), 317 (sh) (268), 331 (sh) (226) and 352 (176). $\tilde{\nu}_{max}$/cm^{-1} 3352s, 1662m, 1597s, 1437s, 1361m, 1140m, 1023m and 752m (paraffin). δ_H ($CDCl_3$) 3.89 (6 H, s, $3CH_2$), 4.72 (2 H, s, CH_2), 7.07–7.12 (3 H, m, 3 H of C_5H_3N), 7.39 (1 H, d, J = 8.2 Hz, 1 H of C_5H_3N), 7.52–7.62 (5 H, m, 5 H of C_5H_3N) and 8.53 (2 H, d, J = 5.1 Hz, 2 H of C_5H_3N).

Bis[6-(hydroxymethyl)-2-pyridylmethyl](2-pyridylmethyl)-amine, H_2L^2. A solution of 6-(bromomethyl)-2-(hydroxymethyl)pyridine[17] (0.903 g, 4.47 mmol) in acetonitrile (50 mL) was treated slowly with a solution of (2-pyridylmethyl)amine (0.230 mL, 2.23 mmol) and triethylamine (0.622 mL, 4.47 mmol) in acetonitrile (25 mL) under a dinitrogen atmosphere. The pink solution turned orange and was stirred. A white precipitate began to appear after 18 h. Stirring was continued for 12 h, whereupon the white precipitate was filtered off and the solvent removed using a rotary evaporator to yield a pale orange solid. This was dissolved in chloroform and washed with saturated $NaHCO_3$ then brine solutions. The chloroform layer was dried over anhydrous magnesium sulfate, filtered and the solvent evaporated from the filtrate to give a light brown oil (0.450 g, 58%). Larger scale preparations increased the yield to 75%. EI-MS: *m*/*z* (351 (MH^+, 8%), 258 [($M - CH_2C_5H_4N)^+$ 60] and 228 [($M - CH_2C_5H_3NCH_2OH)^+$, 100]. λ_{max}/nm(CH_3CN) 264 (ε/dm^3 mol^{-1} cm^{-1} 9910) and 278 (sh) (6561); δ_H ($CDCl_3$) 3.87 (6 H, s, $3CH_2$), 4.73 (4 H, s, $2CH_2$), 7.06 (3 H, d, J = 7.2, 3 H of C_5H_3N), 7.24 (2 H, t, J = 6.1, 2 H of C_5H_3N), 7.39 (1 H, d, J = 7.2, 1 H of C_5H_3N), 7.58–7.65 (4 H, m, 4 H of C_5H_3N) and 8.53 (1 H, d, J = 4.1 Hz, H of C_5H_3N): $\tilde{\nu}_{max}$/cm^{-1} (paraffin) 3300s, 1687s, 1458s, 1385m, 1366m, 997m and 685m.

Tris[6-(hydroxymethyl)-2-pyridylmethyl]amine, H_3L^3. A solution of 6-(bromomethyl)-2-(hydroxymethyl)pyridine[17] (2.0 g, 10 mmol) in acetonitrile (20 mL) was stirred with ammonium acetate (0.25 g, 3.3 mmol) and ground sodium carbonate (0.70 g, 6.6 mmol) under a dinitrogen atmosphere. Additional ground sodium carbonate (250 mg) was added after 3 days. The reaction was monitored by ^{1}H NMR spectroscopy and stopped when the starting material was no longer apparent in the reaction mixture. The mixture was filtered and the acetonitrile solution evaporated to yield a white solid which was purified by flash chromatography (silica gel support; eluent dichloromethane–methanol gradient). A single band was obtained that gave the product, a clear white solid, on evaporation and drying *in vacuo* (0.8 g), mp 158–160 °C. ES-MS: *m*/*z* 403 [($M+Na)^+$, 60%] and 381 (MH^+, 100). λ_{max}/nm (methanol) 266 (ε/dm^3 mol^{-1} cm^{-1} 11400): δ_H(DMSO) 3.74 (6 H, s, $3CH_2$), 4.52 (6 H, d, J = 5.1, $3CH_2$), 5.34 (3 H, br, 3OH), 7.30 (3 H, d, J = 7.7, 3 H of C_5H_3N), 7.44 (3 H, d, J = 7.7, 3 H of C_5H_3N) and 7.76 (3 H, t, J = 7.7 Hz, 3 H of C_5H_3N). $\tilde{\nu}_{max}$/cm^{-1} (KBr disc) 3368w, 1578s, 1454s, 1153 (sh) and 1053s.

[6-Formyl-2-pyridylmethyl]bis(2-pyridylmethyl)amine. A mixture of dichloromethane (25 mL) and oxalyl chloride (1.0 mL, 11 mmol) was placed in a 100 mL four-necked flask equipped with an overhead mechanical stirrer, a thermometer,

a calcium sulfate drying tube, and two pressure-equalising dropping funnels, one containing dimethyl sulfoxide (1.7 mL, 22 mmol) diluted with dichloromethane (5 mL) and the other HL^1 (0.32 g, 10 mmol) in 10 mL dichloromethane with minimum dimethyl sulfoxide (a few drops) added to dissolve the alcohol. The dimethyl sulfoxide–dichloromethane was added to the stirred oxalyl chloride solution at −50 to −60 °C. The reaction mixture was stirred for 2 min and then HL^1 added over 5 min. The mixture was stirred at −50 to −60 °C for 15 min and then triethylamine (7.0 mL, 50 mmol) added. After stirring for 5 min the mixture was slowly warmed to room temperature. Water (50 mL) was added and the organic and aqueous layers were separated. The aqueous layer was extracted with dichloromethane (2 × 25 mL). The organic layers were combined, washed with saturated sodium chloride solution (100 mL) and dried over magnesium sulfate. Removal of the solvent under vacuum yielded the product, a pale brown oil (0.304 g, 95%). EI-MS: *m/z* 319 (MH^+, 100). δ_H ($CDCl_3$) 3.92 (4 H, s, $2CH_2$), 3.99 (2 H, s, CH_2), 7.11–7.16 (2 H, m, 2 H of C_5H_3N), 7.55 (2 H, d, $J = 8.2$, 2 H of C_5H_3N), 7.64 (2 H, m, 2 H of C_5H_3N), 7.80 (3 H, m, 3 H of C_5H_3N), 8.53 (2 H, d, $J = 5.1$ Hz, 2 H of C_5H_3N) and 10.04 (1 H, s, CHO). $\tilde{\nu}_{max}/cm^{-1}$ (paraffin) 2939m, 1710s, 1607m, 1588m, 1514m, 1456s, 1242s, 1181s, 1128m, 1049m, 1027m, 966s, 924m, 871m and 798m.

[2-(6-Chloromethyl)pyridylmethyl]bis(2-pyridylmethyl)amine. A solution of $SOCl_2$ (1 mL) in dry $CHCl_3$ (10 mL) was added to a solution of HL^1 (0.110 g, 0.34 mmol) in dry $CHCl_3$ (10 mL) chilled to −5 °C with an ethanol–ice bath. The khaki reaction mixture was warmed to room temperature and was kept at this temperature overnight. The volatiles were evaporated under high vacuum leaving an oily greenish residue that was dissolved in THF (50 mL) containing triethylamine (4.4 mL). Some solid precipitated and was filtered off. The solvent was removed and the brownish oily residue flash chromatographed (neutral alumina support; eluent 10% methanol in chloroform). The single pale yellow band gave a pale yellow solid (0.51 g, 50%), mp 91–92 °C (Found: C, 66.76; H, 5.71; N, 16.58. Calc. for $C_{19}H_{19}ClN_4$: C, 67.35; H, 5.65; N, 16.53%). ES-MS: *m/z* 338 (M^+, 8%). δ_H ($CDCl_3$) 3.88 (6 H, s, $3CH_2$), 4.61 (2 H, s, CH_2), 7.08–7.13 (2 H, m, 2 H of C_5H_3N), 7.30 (1 H, m, 1 H of C_5H_3N), 7.4–7.7 (6 H, m, 6 H of C_5H_3N) and 8.50 (2 H, d, $J = 4.6$ Hz, 2 H of C_5H_3N).

[Cu(HL^1)Cl]Cl 1. A solution of HL^1 (0.110 g, 0.34 mmol) in methanol (10 mL) was added dropwise to a green solution of copper(II) chloride (0.059 g, 0.34 mmol) in methanol (3 mL). A deep sky blue colour developed immediately. The solution was left to stand for several days under a diethyl ether atmosphere. A blue solid precipitated and was collected by filtration, washed several times with diethyl ether and dried with a dinitrogen flow, mp 112 °C (decomp.) (Found: C, 49.92; H, 4.36; N, 12.32. $C_{19}H_{20}Cl_2CuN_4O$ requires C, 50.16; H, 4.40; N, 12.11%). ES-MS: *m/z* 420 {[CuCl(HL^1)]$^+$, 8%} and 382 {[Cu(HL^1)]$^+$, 100}. λ_{max}/nm (methanol) 258 (ε/dm^3 mol^{-1} cm^{-1} 10800), 723 (85) and 880 (80). EPR (MeOH glass, 77 K): $g_\parallel = 2.24$, $g_\perp = 2.04$, $A_\parallel = 148$ G. $\tilde{\nu}/cm^{-1}$ (KBr disc) 3224m, 3075m, 3038m, 3000w, 2924m, 1597s, 1587m, 1494m, 1454s, 1445m, 1358w, 1304w, 1281m, 1248w, 1096w, 1062s, 1052m, 1026m, 986m, 882m, 780s and 763m. Λ_M (10^{-3} M in DMF) 50 S cm^2 mol^{-1}.

[Cu(H_2L^2)Cl]Cl 2. To a solution of H_2L^2 (0.100 g, 0.285 mmol) in methanol (10 mL) was added dropwise a green solution of copper(II) chloride (0.048 g, 0.283 mmol) in methanol (3 mL). The yellow solution of the ligand immediately became deep blue. This was left to stand under a diethyl ether atmosphere. The blue crystals which formed were collected using a pipette, washed several times with diethyl ether and dried with a nitrogen flow (0.050 g, 36%), mp 180 °C (decomp.) (Found: C, 47.72; H, 4.70; N, 11.06. $C_{20}H_{22}Cl_2CuN_4O_2 \cdot H_2O$ requires C, 47.76; H, 4.77; N, 11.14%). ES-MS: *m/z* 470 {[Cu(H_2L^2)(OAc) + H]$^+$, 4%}, 448 {[CuCl(H_2L^2)]$^+$, 8%} and 412 {[Cu(H_2L^2)]$^+$, 100}. λ_{max}/nm (methanol) 260 (ε/dm^3 mol^{-1} cm^{-1} 15000), 714 (120) and 860 (90). EPR (MeOH glass, 77 K): $g_\parallel = 2.24$, $g_\perp = 2.03$, $A_\parallel = 172$ G. $\tilde{\nu}/cm^{-1}$ (KBr disc) 3200vs, 2930w, 1607s, 1576m, 1465m, 1437s, 1280m, 1154m, 1077s, 1052m, 900m, 795m, 780m and 771s. Λ_M (10^{-3} M in DMF) 48 S cm^2 mol^{-1}.

[Cu(H_2L^2)Cl][OTs] 3. Sodium *p*-toluenesulfonate (0.200 g) in methanol (20 mL) was added to a dark blue solution of H_2L^2 (0.310 g, 0.884 mmol) and copper(II) chloride (0.120 g, 0.885 mmol) in methanol (10 mL). After 30 min, the solvent volume was reduced (to *ca.* 10 mL) and diethyl ether added until precipitation commenced. The reaction mixture was cooled and the resulting bright blue precipitate collected by filtration. Recrystallisation from methanol under a diethyl ether atmosphere afforded clear blue, block-shaped crystals (0.086 g, 17%), mp 267–270 °C (decomp.) (Found: C, 52.35; H, 4.62; N, 8.96. $C_{27}H_{29}ClCuN_4O_5S$ requires C, 52.25; H, 4.71; N, 9.03%). ES-MS: *m/z* (639 ({[Cu(H_2L^2)Cl] + OTs}$^+$, 2%), 448 {[Cu(H_2L^2)Cl]$^+$, 10} and 412 {[Cu(H_2L^2)]$^+$, 100}. λ_{max}/nm (CH_3CN) 261 (ε/dm^3 mol^{-1} cm^{-1} 15200), 700 (185) and 902 (sh) (160). EPR (MeOH glass, 77 K): $g_\parallel = 2.34$, $g_\perp = 2.06$, $A_\parallel = 111$ G. $\tilde{\nu}/cm^{-1}$ (KBr disc) 3351s, 2920w, 1605s, 1578m, 1438s, 1206s, 1129m, 1082m, 1064m, 1037m, 1013m, 816m and 689m.

[Cu(L^2BF_2)][BF_4] 4. A pale blue solution of Cu[BF_4]$_2 \cdot n H_2O$ (0.32 g at ≈20% Cu, ≈1.0 mmol) in acetonitrile (25 mL) was added *via* cannula to a yellow solution of H_2L^2 (0.47 g, 1.33 mmol) in acetonitrile (25 mL). A deep sky blue solution formed. The solvent was reduced to 15 mL and, after standing for several days under a diethyl ether atmosphere, blue crystals were obtained. These were recrystallised from acetonitrile under a diethyl ether atmosphere to give bright blue needles (0.208 g, 28%), mp 252–254 °C (Found: C, 43.79; H, 3.54; N, 9.84. $C_{20}H_{20}B_2CuF_6N_4O_2$ requires C, 43.87; H, 3.68; N, 10.23%). ES-MS: *m/z* 550 {[Cu(L^2BF_2)][BF_4]$^+$, 5%}, 460 {[Cu(L^2BF_2)]$^+$, 100} and 412 {Cu(L^2)$^+$, 35}. λ_{max}/nm (CH_3CN) 260 (ε/dm^3 mol^{-1} cm^{-1} 16900), 690 (135) and 804 (175). $\tilde{\nu}/cm^{-1}$ (KBr disc) 3408s, 2959w, 1605m, 1465m, 1439m, 1123m, 1083s and 1035s. EPR (MeOH glass, 77 K): $g_\parallel = 2.25$, $g_\perp = 2.07$, $A_\parallel = 160$ G. Λ_M (10^{-3} M in DMF) 70 S cm^2 mol^{-1}.

[Cu(H_3L^3)$Br_{0.43}Cl_{0.57}$]$_2$[Cu($Br_{0.43}Cl_{0.57}$)$_2$($Br_{0.97}Cl_{0.03}$)$_2$] 5. To a colourless solution of $H_3L^3 \cdot x$NaBr (20 mg) in methanol a green solution of $CuCl_2 \cdot 2H_2O$ (8.9 mg) in methanol (1 mL) was added. A dark green solution formed immediately. This was left to stand under a diethyl ether atmosphere for several days. Over this time the solution gradually turned brown and an oily brown solid precipitated. This was taken up in the minimum of anhydrous tetrahydrofuran and placed under a diethyl ether atmosphere. A mixture of brown and green crystals formed. Several small brown crystals were manually isolated from the mixture using a microscope. ES-MS: *m/z* 444 {[Cu(H_3L^3)]$^+$, 85%} and 222 {[Cu(H_3L^3)]$^{2+}$, 100}. λ_{max}/nm (methanol) 260 (ε/dm^3 mol^{-1} cm^{-1} 11030), 820 (80), 1098 (55) and 1410 (25). $\tilde{\nu}/cm^{-1}$ (KBr disc) 3366s, 1601s, 1573m, 1469m, 1450s, 1159m, 1077s, 1059s, 1018s, 1003m, 789m and 779m. The stoichiometry given for the compositionally disordered bromo and chloro ligands is that determined by a crystal structure analysis (see below).

[Cu(H_3L^3)Br]Br 6. The compound $CuBr_2$ (11 mg) in THF (1 cm^3) was added to $H_3L^3 \cdot x$NaBr (26 mg) in methanol (3 mL) to give a clear grass green solution which was left to stand under a diethyl ether atmosphere for three days. Green-blue block-shaped crystals formed. The crystals were collected using a pipette, washed several times with diethyl ether and dried with a nitrogen stream (9.5 mg, 32%), mp 160 °C (decomp.) (Found: C, 41.95; H, 4.06; N, 9.26. $C_{21}H_{24}Br_2CuN_4O_3$ requires C, 41.77;

Table 6 Numerical crystal and refinement data for the structures **1–7** determined by X-ray crystallography at 294 K

	1	**2**	**3**	**4**	**5**	**6**	**7**
Formula	$C_{19}H_{20}Cl_2CuN_4O$	$C_{20}H_{22}Cl_2CuN_4O_2$	$C_{27}H_{29}ClCuN_4O_5S$	$C_{20}H_{20}B_2CuF_6N_4O_2$	$C_{21}H_{24}Br_{1.83}Cl_{1.18}Cu_{1.5}N_4O_3$	$C_{21}H_{24}Br_2CuN_4O_3$	$C_{48}H_{61}B_2BrCu_3F_8N_8O_{7.5}$
M	454.8	484.9	620.6	547.6	663.0	603.8	1314.2
Crystal system	Monoclinic	Monoclinic	Triclinic	Monoclinic	Monoclinic	Orthorhombic	Monoclinic
Space group	*C*2/*c*	$P2_1/c$	$P\bar{1}$	$P2_1/c$	*C*2/*c*	*Pbca*	$P2_1/n$
a/Å	20.669(9)	8.204(5)	8.929(5)	9.206(5)	16.310(4)	16.793(3)	14.600(3)
b/Å	13.190(3)	16.174(3)	12.006(7)	20.410(4)	10.311(1)	14.003(2)	19.021(4)
c/Å	15.770(7)	16.453(9)	14.098(9)	13.364(7)	28.039(6)	18.986(3)	19.560(3)
α/°			114.43(3)				
β/°	112.92(2)	105.85(2)	97.71(4)	119.44(2)	90.77(1)		90.407(8)
γ/°			91.00(4)				
V/Å^3	3960(3)	2100(2)	1359(1)	2187(2)	4715(2)	4465(2)	5432(2)
Z	8	4	2	4	8	8	4
μ/cm^{-1}	13.93 (Mo-Kα)	13.21 (Mo-Kα)	10.20 (Mo-Kα)	10.75 (Mo-Kα)	69.34 (Cu-Kα)	58.63 (Cu-Kα)	29.45 (Cu-Kα)
Reflections collected	3595	2850	4988	4009	3577	4222	5860
R_{int} (no. equiv. reflections)	0.016 (101)	0.015 (112)	0.012 (214)	0.019 (175)	0.013 (80)	— (nil)	0.027 (279)
Observed reflections [$I/\sigma(I) > 3$]	2625	1826	3593	2498	2291	3148	3579
Final R, R_w [$I/\sigma(I) > 3$]	0.027, 0.042	0.029, 0.039	0.031, 0.042	0.048, 0.059	0.026, 0.038	0.031, 0.040	0.062, 0.091

H, 4.01; N, 9.28%); ES-MS: *m*/*z* 443 and 442 {$[Cu(H_3L^3)]^+$, 100%}. λ_{max}/nm (dichloromethane) 262 (ε/dm^3 mol^{-1} cm^{-1} 9840) and 780 (185). EPR (dichloromethane glass, 77 K): $g_\parallel = 2.249$, $g_\perp = 2.095$, $A_\parallel = 146$ G. $\tilde{\nu}$/cm^{-1} (KBr disc) 3445s, 1609m, 1439m, 1152m, 1083s and 1035s.

$[Cu_3\{H_3(L^3)_2\}][BF_4]_2$ 7. A green solution of $Cu[BF_4]_2{\cdot}nH_2O$ (12.5 mg) in methanol (1 mL) was transferred by a cannula to a colourless solution of $H_3L^3{\cdot}x$NaBr (20 mg) in methanol (3 mL). A deep green-blue solution immediately formed. This was stood under a diethyl ether atmosphere for several days. A purple oil formed which was recrystallised from 4 : 1 *n*-butanol–tetrahydrofuran. Slow evaporation afforded several small green crystals of the product. ES-MS: *m*/*z* 515 {$[Cu_3Br\{(H_3(L^3)_2\}]^{2+}$, 4%}, 444 {$[Cu(H_3L^3)]^+$, 85} and 222 {$[Cu(H_3L^3)]^{2+}$, 100}. λ_{max}/nm(methanol) 262 (ε/dm^3 mol^{-1} cm^{-1} 24800), 703 (290) and 1120 (110). EPR (MeOH glass, 77 K): sub-spectrum 1 (1 Cu) $g_\parallel = 2.27$, $A_\parallel = 126$ G, $g_\perp \approx 2.03$ and sub-spectrum 2 (2 Cu) $g_\parallel = 2.18$, $A_\parallel = 150$ G, $g_\perp \approx 2.07$.

X-Ray crystallography

Crystal and refinement data for complexes **1**–**6** are listed in Table 6. For **4** the $[BF_4]^-$ ion was considerably disordered and modelled as three independently refinable but identical rigid bodies, with the sum of their occupancies equal to 1.0; the remaining non-hydrogen atoms were refined with individual positional and anisotropic thermal parameters. Complex **5** has compositionally disordered bromide and chloride ligands and refined as $[Cu(H_3L^3)Br_{0.43}Cl_{0.57}]_2[Cu(Br_{0.43}Cl_{0.57})_2(Br_{0.97}Cl_{0.03})_2]$. Complex **7** refines as $[Cu_3\{H_3(L^3)_2\}Br][BF_4]_2{\cdot}0.5C_4H_9OH{\cdot}$thf. Whilst the $[Cu_3\{H(L^3)_2\}]Br]^{2+}$ ion is well defined in the structure, the $[BF_4]^-$ ions, the 1-butanol and the thf molecules are positionally disordered and were each modelled as two independently refinable bodies.

CCDC reference number 186/1898.

See http://www.rsc.org/suppdata/dt/b0/b000092m/ for crystallographic files in .cif format.

Acknowledgements

We thank the Australian Research Council for financial support.

References

1 H. C. Liang, M. Dahan and K. D. Karlin, *Curr. Opin. Chem. Biol.*, 1999, **3**, 168.
2 L. Que, Jr. and Y. Dong, *Acc. Chem. Res.*, 1996, **29**, 190; H.-F. Hsu, Y. Dong, L. Shu, V. G. Young, Jr. and L. Que, Jr., *J. Am. Chem. Soc.*, 1999, **121**, 5230 and references therein.
3 P. A. Goodson, A. R. Oki, J. Glerup and D. J. Hodgson, *J. Am. Chem. Soc.*, 1990, **112**, 6254; J. E. McGrady and R. Stranger, *J. Am. Chem. Soc.*, 1997, **119**, 8512; A. Diebold and K. S. Hagen, *Inorg. Chem.*, 1998, **37**, 215.
4 K. D. Karlin, S. Kaderli and A. D. Zuberbuhler, *Acc. Chem. Res.*, 1997, **30**, 139; K. D. Karlin, D. H. Lee, H. V. Obias and K. J. Humphries, *Pure Appl. Chem.*, 1998, **70**, 855.
5 G. Anderegg and F. Wenk, *Helv. Chim. Acta*, 1967, **50**, 2330; G. Anderegg, E. Hubmann, N. G. Podder and F. Wenk, *Helv. Chim. Acta*, 1977, **60**, 123; M. Harata, K. Jitsukawa, H. Masuda and H. Einaga, *J. Am. Chem. Soc.*, 1994, **116**, 10817; K. D. Karlin, A. Nanthakumar, S. Fox, N. N. Murthy, N. Ravi, B. H. Huynh, R. D. Orosz and E. P. Day, *J. Am. Chem. Soc.*, 1994, **116**, 4753; I. Sanyal, P. Ghosh and K. D. Karlin, *Inorg. Chem.*, 1995, **34**, 3050; N. Komeda, H. Nagao, Y. Kushi, G. Adachi, M. Suzuki, A. Uehara and K. Tanaka, *Bull. Chem. Soc. Jpn.*, 1995, **68**, 581; L. M. Berreau, S. Mahapatra, J. A. Halfen, V. G. Young, Jr. and W. B. Tolman, *Inorg. Chem.*, 1996, **35**, 6339; S. Fox, A. Nanthakumar, M. Wikstrom, K. D. Karlin and N. J. Blackburn, *J. Am. Chem. Soc.*, 1996, **118**, 24; M. Harata, K. Jitsukawa, H. Masuda and H. Einaga, *Chem. Lett.*, 1996, 814; A. Nanthakumar, S. Fox, N. N. Murthy and K. D. Karlin, *J. Am. Chem. Soc.*, 1997, **119**, 3898; J. W. Canary, C. S. Allen, J. M. Castagnetto, Y. H. Chiu, P. J. Toscano and Y. H.

Wang, *Inorg. Chem.*, 1998, **37**, 6255; M. Harata, K. Jitsukawa, H. Masuda and H. Einaga, *J. Coord. Chem.*, 1998, **44**, 311; *Bull. Chem. Soc. Jpn.*, 1998, **71**, 637; M. Harata, K. Hasegawa, K. Jitsukawa, H. Masuda and H. Einaga, *Bull. Chem. Soc. Jpn.*, 1998, **71**, 1031; M. Costas and A. Llobet, *J. Mol. Catal. A*, 1999, **142**, 113; D. M. Corsi, N. N. Murthy, V. G. Young and K. D. Karlin, *Inorg. Chem.*, 1999, **38**, 848.

6 A. Wada, M. Harata, K. Hasegawa, K. Jitsukawa, H. Masuda, M. Mukai, T. Kitagawa and H. Einaga, *Angew. Chem., Int. Ed.*, 1998, **37**, 798.

7 D. H. Lee, N. Wei, N. N. Murthy, Z. Tyelkar, K. D. Karlin, S. Kalderli, B. Jung and A. Zuberbuhler, *J. Am. Chem. Soc.*, 1995, **117**, 12498.

8 D. H. Lee, N. N. Murthy and K. D. Karlin, *Inorg. Chem.*, 1997, **36**, 5785; J. E. Bol, W. L. Driessen, R. Y. N. Ho, B. Maase, L. Que, Jr. and J. Reedijk, *Angew. Chem., Int. Ed. Engl.*, 1997, **36**, 998; P. Comba, P. Hilfenhaus and K. D. Karlin, *Inorg. Chem.*, 1997, **36**, 2309.

9 H. V. Obias, G. P. Van Strijdonck, D. H. Lee, M. Ralle, N. J. Blackburn and K. D. Karlin, *J. Am. Chem. Soc.*, 1998, **120**, 9696; T. D. Ju, R. A. Ghiladi, D. H. Lee, G. P. Van Strijdonck, A. S. Woods, R. J. Cotter, V. G. Young and K. D. Karlin, *Inorg. Chem.*, 1999, **38**, 2244.

10 C.-L. Chuang, K. Lim, O. dos Santos, X. Xu and J. W. Canary, *Inorg. Chem.*, 1997, **36**, 1967.

11 C.-L. Chuang, K. Lim and J. W. Canary, *Supramol. Chem.*, 1995, **5**, 39.

12 H. Nagao, N. Komeda, M. Mukaida, M. Suzuki and K. Tanaka, *Inorg. Chem.*, 1996, **35**, 6809.

13 N. Wei, N. N. Murthy, Z. Tyeklár and K. D. Karlin, *Inorg. Chem.*, 1994, **33**, 1177; N. Wei, N. N. Murthy, Q. Chen, J. Zubieta and K. D. Karlin, *Inorg. Chem.*, 1994, **33**, 1953.

14 J. P. Klinman, *Chem. Rev.*, 1996, **96**, 2541.

15 E. I. Solomon, U. M. Sundaram and T. E. Machonkin, *Chem. Rev.*, 1996, **96**, 2563.

16 C. Ostermeier, A. Harrenga, U. Ermler and H. Michel, *Proc. Natl. Acad. Sci. U.S.A.*, 1997, **94**, 10547; S. Yoshikawa, K. Shinzawa-Itoh, R. Nakashima, R. Yaono, E. Yamashita, N. Inoue, M. Yao, M. J. Fei, C. P. Libea, T. Mizushima, H. Yamaguchi, T. Tomizaki and T. Tsulihara, *Science*, 1998, **280**, 1723.

17 M. Newcombe, G. W. Gokel and D. J. Cram, *J. Am. Chem. Soc.*, 1974, **96**, 6810; B. Kaptein, G. Barf, R. M. Kellogg and F. V. Bolhuis, *J. Org. Chem.*, 1990, **55**, 1890.

18 H. Toflund and S. Ishiguru, *Inorg. Chem.*, 1989, **28**, 2236; C.-L. Chuang, M. Frid and J. W. Canary, *Tetrahedron. Lett.*, 1995, **36**, 2909.

19 Copper complexes of examples include: R. R. Gagne, J. L. Allison and G. C. Lisensky, *Inorg. Chem.*, 1978, **17**, 3563; O. P. Anderson and A. B. Packard, *Inorg. Chem.*, 1980, **19**, 2123, 2941; N. Aoi, Y. Takano, H. Ogino, G.-E. Matsubayashi and T. Tanaka, *J. Chem. Soc., Chem. Commun.*, 1985, 703; N. Aoi, G.-E. Matsubayashi and T. Tanaka, *J. Chem. Soc., Dalton Trans.*, 1987, 241; M. J. Scott and R. H. Holm, *J. Am. Chem. Soc.*, 1994, **116**, 11357.

20 B. Alpha, E. Anklam, R. Dreschenaux, J.-M. Lehn and M. Piettrakiewicz, *Helv. Chim. Acta*, 1988, **71**, 1042; L. Echegoyen, E. Perez-Cordero, J.-B. Regnouf de Vains, C. Roth and J.-M. Lehn, *Inorg. Chem.*, 1993, **32**, 572 and references therein.

21 A. W. Addison, A. N. Rao, J. Reedijk, J. Rijn and G. C. Verschoor, *J. Chem. Soc., Dalton Trans.*, 1984, 1349.

22 B. J. Hathaway, in *Comprehensive Coordination Chemistry*, ed. G. Wilkinson, Pergamon Press, Oxford, 1987, vol. 5, ch. 53, p. 533.

23 K. D. Karlin, J. C. Hayes, S. Juen, J. P. Hutchinson and J. Zubieta, *Inorg. Chem.*, 1982, **21**, 4106.

24 E. A. Ambundo, M. V. Deydier, A. J. Grall, N. Aguera-Vega, L. T. Dressel, T. H. Cooper, M. J. Heeg, L. A. Ochrymowycz and D. B. Rorabacher, *Inorg. Chem.*, 1999, **38**, 4233.

25 Z. J. Chen, Z. He, N. Karasek, D. C. Craig and S. B. Colbran, unpublished work.

26 WinEPR Simfonia V1.25, Bruker Analytische Messtechnik GmbH, Rheinstetten, 1997.

27 S. B. Sembiring, S. B. Colbran and D. C. Craig, *J. Chem. Soc., Dalton Trans.*, 1999, 1543.